

Meson Mass Decomposition from Lattice QCD

Yi-Bo Yang^{1,2}, Ying Chen¹, Terrence Draper², Ming Gong^{1,2}, Keh-Fei Liu², Zhaofeng Liu¹, and Jian-Ping Ma^{3,4}



(χQCD Collaboration)

¹*Institute of High Energy Physics, Chinese Academy of Sciences, Beijing 100049, China*

²*Department of Physics and Astronomy, University of Kentucky, Lexington, KY 40506*

³*State Key Laboratory of Theoretical Physics, Institute of Theoretical Physics, Chinese Academy of Sciences, Beijing 100190, China*

⁴*Center for High Energy Physics, Peking University, Beijing 100871, China*

Hadron masses can be decomposed as a sum of quark and glue components which are defined through hadronic matrix elements of QCD operators. The components consist of the quark mass term, the quark energy term, the glue energy term, and the trace anomaly term. We calculate these components for mesons with lattice QCD for the first time. The calculation is carried out with overlap fermion on 2 + 1 flavor domain-wall fermion gauge configurations. We confirm that $\sim 50\%$ of the light pion mass comes from the quark mass term and $\sim 10\%$ comes from the quark energy; whereas, while for the ρ meson, the quark energy contributes roughly half of its mass but the quark mass term contributes little. The combined glue components contribute $\sim 40 - 50\%$ for both mesons. It is interesting to observe that the quark mass contribution to the mass of the vector meson is almost linear in quark mass over a large quark mass region below the charm quark mass. For heavy mesons, the quark mass term dominates the masses, while the contribution from the glue components is about 200 MeV (a bare value around 2 GeV) for the heavy pseudoscalar and vector mesons. The charmonium hyperfine splitting is found to be dominated by the quark energy term which is consistent with the picture of the quark potential model.

PACS numbers: 11.15.Ha, 12.38.Gc, 12.39.Mk

I. INTRODUCTION

Hadrons are confined states of quarks and gluons. QCD is the theory describing the interaction of the quarks and gluons. Given the fact that masses of hadrons are well measured and successfully calculated with lattice QCD, an interesting, important, and yet unanswered question is how large are the contributions to the masses from the quark and glue constituents. The answer will be important for understanding the quark-gluon structure of hadrons. It is clear that the question can only be answered by solving QCD nonperturbatively, and/or with information from experiment. The decomposition for the proton has been carried out with phenomenological inputs [1]. For hadrons other than the proton, there is little information from experiments to be used, while some discussion is provided in [2, 3]. At the same time, the question can be addressed for all the hadrons by employing lattice QCD. In this paper, we present such an exploratory study with lattice QCD calculations for the pseudoscalar (PS) and vector (V) mesons.

The energy-momentum tensor from the QCD Lagrangian in Euclidean space [4] is

$$T_{\mu\nu} = \frac{1}{4}\bar{\psi}\gamma_{(\mu}\overleftrightarrow{D}_{\nu)}\psi + F_{\mu\alpha}F_{\nu\alpha} - \frac{1}{4}\delta_{\mu\nu}F^2, \quad (1)$$

which is symmetric and conserved. Each term in the tensor depends on the renormalization scale, but the total tensor does not. The trace term of the tensor is given by

$$T_{\mu\mu} = -m\bar{\psi}\psi - \gamma_m m\bar{\psi}\psi + \frac{\beta(g)}{2g}F^2, \quad (2)$$

in which the quantum trace anomaly (the term proportional to the anomalous dimension of the mass operator γ_m , plus the glue term) has been taken into account. In the above anomaly equation, the first term and the combined second and third terms are scale independent. The definition of the anomalous dimension of the mass operator is [5],

$$\gamma_m = -\frac{\mu}{m} \frac{dm}{d\mu}. \quad (3)$$

In lowest order perturbation, the coefficient of the glue anomaly term (the third term in Eq. (2)) is $\beta(g) = -(11 - 2n_f/3)g^3/(4\pi)^2$ with n_f being the number of flavors.

Combining the classical $T_{\mu\nu}$ from Eq. (1) and the quantum anomaly in Eq. (2), one can divide $T_{\mu\nu}$ into a traceless part $\hat{T}_{\mu\nu}$ and a trace part $\hat{T}_{\mu\nu}$, i.e. $T_{\mu\nu} = \bar{T}_{\mu\nu} + \hat{T}_{\mu\nu}$ [1]. From its matrix element of a single-meson state

with momentum P , $\langle P|T_{\mu\nu}|P\rangle = 2P_\mu P_\nu$, and taking $\mu = \nu = 4$ in the rest frame, one has

$$\begin{aligned}\langle T_{44}\rangle &\equiv \frac{\langle P|\int d^3x T_{44}(\vec{x})|P\rangle}{\langle P|P\rangle} = -M, \\ \langle \bar{T}_{44}\rangle &= -3/4M, \quad \langle \hat{T}_{44}\rangle = -1/4M,\end{aligned}\quad (4)$$

with

$$\begin{aligned}\bar{T}_{44} &= \frac{1}{4}\bar{\psi}\gamma_{(4}\overleftrightarrow{D}_{4)}\psi - \frac{1}{16}\bar{\psi}\gamma_{(\mu}\overleftrightarrow{D}_{\mu)}\psi \\ &\quad + F_{4\alpha}F_{4\alpha} - \frac{1}{4}F^2 \\ &= \sum_{u,d,s}(\bar{\psi}\gamma_4\overleftrightarrow{D}_4\psi + \frac{1}{4}m\bar{\psi}\psi) + \frac{1}{2}(E^2 - B^2), \quad (5) \\ \hat{T}_{44} &= \frac{1}{4}T_{\mu\mu} \\ &= \frac{1}{4}[-(1 + \gamma_m) \sum_{u,d,s,\dots} m\bar{\psi}\psi + \frac{\beta(g)}{g}(E^2 + B^2)],\end{aligned}\quad (6)$$

for the zero momentum case. The Hamiltonian of QCD can be decomposed as [1]

$$\begin{aligned}H_{QCD} &\equiv -\int d^3x T_{44}(\vec{x}) = H_q + H_g + H_g^a + H_m^\gamma, \quad (7) \\ H_q &= -\sum_{u,d,s,\dots} \int d^3x \bar{\psi}(D_4\gamma_4)\psi, \\ H_g &= \int d^3x \frac{1}{2}(B^2 - E^2), \\ H_g^a &= \int d^3x \frac{-\beta(g)}{4g}(E^2 + B^2), \\ H_m^\gamma &= \sum_{u,d,s,\dots} \int d^3x \frac{1}{4}\gamma_m m \bar{\psi}\psi\end{aligned}\quad (8)$$

with H_q , H_g , H_g^a , and H_m^γ denoting the total contributions from the quarks, the glue field energy, the QCD glue trace anomaly, and the quark mass anomaly, respectively. Note that the sum of the first two and the sum of the last two terms are separately scale and renormalization scheme independent, while each term separately is not. Using the equation of motion (EOM), H_q can be further divided into quark energy and mass terms

$$H_q = H_E + H_m, \quad (9)$$

with

$$\begin{aligned}H_E &= \sum_{u,d,s,\dots} \int d^3x \bar{\psi}(\vec{D} \cdot \vec{\gamma})\psi, \\ H_m &= \sum_{u,d,s,\dots} \int d^3x m \bar{\psi}\psi.\end{aligned}\quad (10)$$

N.B.: the quark energy H_E includes both kinetic and potential energies due to the covariant derivative. Given

the above division, a hadron mass can be decomposed into the following matrix elements,

$$\begin{aligned}M &= -\langle T_{44}\rangle = \langle H_q\rangle + \langle H_g\rangle + \langle H_a\rangle + \langle H_m^\gamma\rangle \\ &= \langle H_E\rangle + \langle H_m\rangle + \langle H_g\rangle + \langle H_a\rangle,\end{aligned}\quad (11)$$

$$\frac{1}{4}M = -\langle \hat{T}_{44}\rangle = \langle H_m\rangle + \langle H_a\rangle, \quad (12)$$

with all the $\langle H\rangle$ defined by $\langle P|H|P\rangle/\langle P|P\rangle$ and

$$\langle H_a\rangle = \langle H_m^\gamma\rangle + \langle H_g^a\rangle \quad (13)$$

as the total trace anomaly. Each matrix element can be calculated with lattice QCD. Since hadron masses can be obtained from the two-point correlators on the lattice, we shall calculate $\langle H_q\rangle$ (or $\langle H_E\rangle$) and $\langle H_m\rangle$ through the three-point correlators and extract $\langle H_a\rangle$ and $\langle H_g\rangle$ from Eqs. (11) and (12) in this work. We will directly calculate these glue matrix elements in the future.

The structure of the rest of the paper is organized as follows. The numerical details of the simulation, including the fermion action and configurations used, and the systematic uncertainties, will be discussed in Sec. II. In Sec. III, the results such as the condensates in the mesons, the decomposition of the PS/V mesons and their difference (the splitting) are provided. A short summary and outlook are presented in Sec. IV.

II. NUMERICAL DETAILS

In this work, we use the valence overlap fermion on $2+1$ flavor domain-wall fermion (DWF) configurations [6] to carry out the calculation [7]. The effective quark propagator of the massive overlap fermion is the inverse of the operator $(D_c + m)$ [10, 11], where D_c is chiral, i.e. $\{D_c, \gamma_5\} = 0$ [12], and is expressed in terms of the overlap operator D_{ov} as

$$D_c = \frac{\rho D_{ov}}{1 - D_{ov}/2} \text{ with } D_{ov} = 1 + \gamma_5 \epsilon(\gamma_5 D_w(\rho)), \quad (14)$$

where ϵ is the matrix sign function and D_w is the Wilson Dirac operator with a negative mass characterized by the parameter $\rho = 4 - 1/2\kappa$ for $\kappa_c < \kappa < 0.25$. We set $\kappa=0.2$ which corresponds to $\rho = 1.5$.

The lattice we use has a size $24^3 \times 64$ with lattice spacing $a^{-1} = 1.77(5)$ GeV set by Ref. [13]. The light sea u/d quark mass $m_l a = 0.005$ corresponds to $m_\pi \sim 330$ MeV. We have calculated the PS and V meson masses and the corresponding $\langle H_m\rangle$, $\langle H_q\rangle$, and $\langle H_E\rangle$ at 12 valence quark mass parameters which correspond to the renormalized masses $m_q^R \equiv m_q^{\overline{\text{MS}}}(2\text{GeV})$ ranging from 0.016 to 1.1 GeV after the non-perturbative renormalization procedure in Ref. [14]. The smallest one is slightly smaller than the sea quark mass and corresponds to a pion mass at 281 MeV, and the largest quark mass is close to that of the charm. In order to enhance the signal-to-noise ratio in the calculation of three-point functions, we set two smeared noise

grid sources at $t_i = 0/32$ [15] and four noise-grid point sources at positions t_f which are 10 time-slices away from the sources on 101 configurations. To obtain a better signal in the light quark region (<0.1 GeV), the low mode substitution technique [7] is applied to the contraction in those cases.

It would be ideal to use the conserved lattice stress tensor and there are attempts to construct the conserved stress tensor on the lattice perturbatively and non-perturbatively [4] and recently by Suzuki [8, 9] with Wilson flow at finite lattice spacing. However, these approaches inevitably involve complicated sets of operators, which are difficult to compute in the lattice calculation. Our approach is to use the quark stress operators with lattice derivative (the point-split operators with gauge links [4]) for $\bar{\psi}\gamma_\mu\overleftrightarrow{D}_\nu\psi$,

$$\begin{aligned} & \frac{1}{2} (\bar{\psi}(x)\gamma_\mu(U_\nu(x)\psi(x+\hat{\nu}) - U_\nu^\dagger(x-\hat{\nu})\psi(x-\hat{\nu})) \\ & + (\bar{\psi}(x+\hat{\nu})U_\nu(x+\hat{\nu}) - \bar{\psi}(x+\hat{\nu})U_\nu^\dagger(x))\gamma_\mu\psi(x)) \\ & = a\gamma_\mu(x)\overleftrightarrow{D}_\nu\psi(x) + O(a^3), \end{aligned} \quad (15)$$

to carry out lattice calculation at a finite cutoff and then to extrapolate to the continuum limit as a next step.

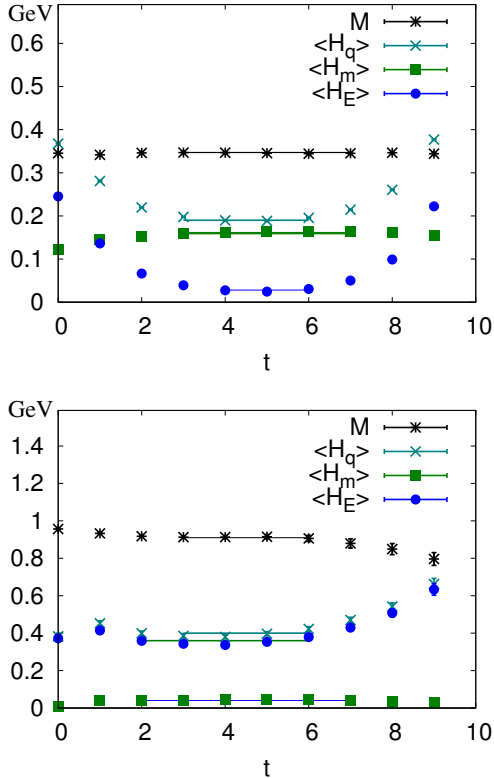


FIG. 1: Plateaus of quark components of (a) PS mesons and (b) V mesons with light quark pairs which correspond to $m_\pi \sim 330$ MeV. Half of each of the light PS/V meson masses comes from the glue, while the other half is dominated by the quark mass/energy in the PS/V case respectively.

The matrix elements for the operators $\bar{\psi}\gamma_4\overleftrightarrow{D}_4\psi$, $\bar{\psi}\gamma_i\overleftrightarrow{D}_i\psi$ and $m\bar{\psi}\psi$ are extracted from the plateaus of the ratios of three-to-two point functions to obtain $\langle H_m \rangle$, $\langle H_q \rangle$, and $\langle H_E \rangle$ in the connected insertions for different quark masses. In the present work, we only consider the equal-mass case for the quark-antiquark pairs in the mesons.

We show in Fig. 1 the ratio of three- to two-point functions for (a) PS mesons and (b) V mesons with light quark pairs, which corresponds to $m_\pi \sim 330$ MeV. We see that the plateaus for $\langle H_m \rangle$, $\langle H_q \rangle$, $\langle H_E \rangle$ from the ratio of three-to-two point functions are clearly visible. At the same time, the plateaus of the total mass M from the effective mass of the two point function with noise-smeared grid source are also long enough to obtain precise results. We also applied a curve fit including the contribution of excited states to extract the matrix elements and found that the results are consistent with the ones from the constant fit.

As observed in Fig. 1, the quark mass term $\langle H_m \rangle$ contributes about half of the light PS mass, while the quark energy term $\langle H_E \rangle$ is very small. This implies that the other half of the light PS mass comes mainly from the glue. For the light V mass, the combined glue components also contributes roughly one half, while $\langle H_E \rangle$ is dominant in the other half, and $\langle H_m \rangle$ is small.

A. Equation of motion and quark energy

Before presenting our results, we discuss the theoretical underpinning of the equation of motion (EOM) in the context of lattice calculation of three-point functions. In the three-point function with the operator $D_c + m$ inserted at a time different from the meson source and sink, part of the correlator will involve the product of the operator and a quark propagator which has the relation

$$\sum_z (D_c + m)_{(x,z)} \cdot \frac{1}{D_c + m_{(z,y)}} = \delta_{x,y}, \quad (16)$$

where x, y, z denote all the space-time, color and Dirac indices. Since the inserted operator $D_c + m$ is at a different time from that of the source time, $x \neq y$. As a result, the matrix element of $D_c + m$ is zero. For the disconnected insertion (DI), the delta function leads to a constant for the quark loop. Since the uncorrelated part after gauge averaging is to be subtracted, this also gives a null result for $D_c + m$ in the DI. Therefore, the matrix element with the insertion of the $D_c + m$ operator is zero which is just the equation of motion on the lattice for fermions with the quark mass as an additive constant in the fermion propagator. This does not hold straightforwardly for the Wilson fermion where there is an additive mass renormalization and mixing with lower dimensional operators which need to be taken into account.

Since D_{ov} has eigenvalues on a unit circle centered at 1 on the real axis, the eigenvalues of D_c are purely imaginary except the zero modes [11]. This is the same as in

the continuum. Thus, $\bar{\psi}D_c\psi$ approaches $\bar{\psi}\gamma_\mu D_\mu\psi$ with an $\mathcal{O}(a^2)$ error and we thus have $\langle H_q \rangle = \langle H_E \rangle + \langle H_m \rangle + \mathcal{O}(a^2)$ as in the continuum in Eq. (9) modulo an $\mathcal{O}(a^2)$ error.

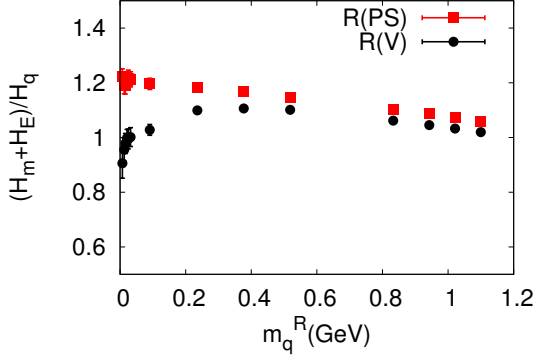


FIG. 2: The ratio R as defined in the text as a function of the renormalized quark mass m_q^R in the \overline{MS} scheme at 2 GeV, to estimate the $\mathcal{O}(a^2)$ error due to the breaking of EOM. The systematic uncertainty vanishes when $R = 1$. The values of R are close to unity except for the very light quark mass region in the PS meson case.

One can estimate this $\mathcal{O}(a^2)$ error by considering the ratio of $\langle D_c \rangle$ to $\langle H_E - H_q \rangle$. Both matrix elements approach the same matrix element of $\bar{\psi}\gamma_\mu \overleftrightarrow{D}_\mu\psi$ in the continuum. This is equivalent to considering the ratio

$$R = \frac{\langle H_m \rangle + \langle H_E \rangle}{\langle H_q \rangle}, \quad (17)$$

which should be equal to $1 + \mathcal{O}(a^2)$. We plot R as a function of the quark mass in Fig. 2 for the PS and V mesons. Except for the region of very light quark masses, they are roughly the same for PS and V mesons. In the charm quark mass region, the ratio is close to unity, while for light quarks, the ratio for the PS can be as large as ~ 1.2 and it is close to unity for the V mesons. We shall take 20% as an conservative estimate for the systematic errors of $\langle H_E \rangle$ and $\langle H_q \rangle$ for the light quark case due to the finite lattice spacing.

B. Disconnected insertion

The DI contribution to the quark mass and quark energy terms needs to be estimated stochastically which is usually quite a bit noisier than that of the connected insertion (CI). It is found recently that the signal of the DI contribution for the quark loops with scalar density can be highly improved by the low-mode averaging (LMA) in the loop and low-mode substitution for the nucleon propagator [15]. We use this approach and calculate the DI of the quark mass term for the PS and V mesons to gauge the DI contributions.

We show the H_m results for the DI in Fig. 3 for the cases where the quark loop mass equals to that of the

light sea (i.e. corresponding to $m_\pi = 330$ MeV), the valence quark mass in the meson, and the strange mass as a function of the valence quark mass of the meson. We see in the upper panel of Fig. 3 that in all cases, the DI contribution of H_m is of the order of a few MeV for all the PS mesons. For the case of the V mesons in the lower panel of Fig. 3, they are also small with the largest contribution being ~ 40 MeV due to the strange quark contribution in the light quark case. It is also about 40 MeV for the case where the the loop and valence has the same quark mass for $m_q > 0.2$ GeV where the vector meson mass is greater than 1.5 GeV. Based on these estimates, we shall ignore the small and noisy DI contribution of H_m in this study.

In view of the fact the strange momentum fraction $\langle x \rangle_s$ is only 2 – 4% of the total nucleon momentum experimentally [16] and the ratio of $\langle x \rangle_s$ to $\langle x \rangle_{u/d}$ in the DI is 0.78(3) from the latest lattice calculation with overlap fermion on DWF configurations on the $24^3 \times 64$ lattice [17], we expect the DI contribution of the quark en-

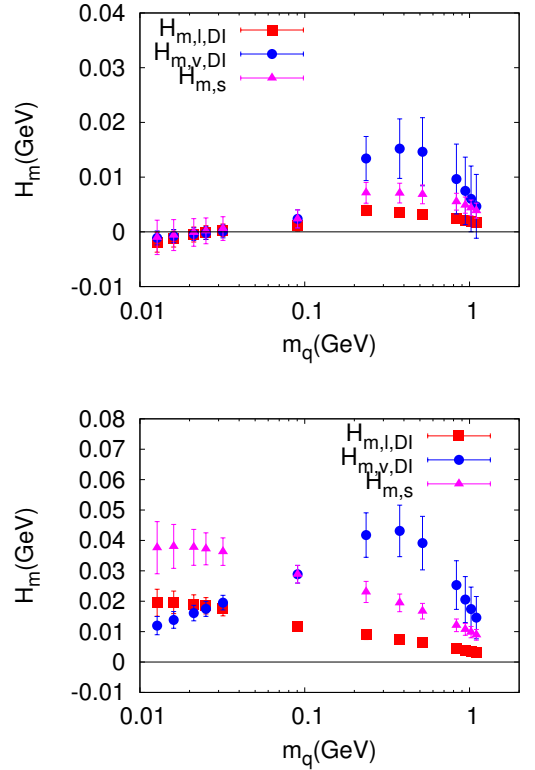


FIG. 3: The contributions of the quark mass term in the PS/V meson from kinds of DI diagrams. The red-square, blue-circle, and pink triangle points are the contributions from the quark loop with mass equal to light sea quark mass, valence quark mass, and strange sea quark mass correspondingly. It is easy to confirm that the DI contribution to the quark mass term in the PS meson case is just a few MeV for all cases, while that in the V meson case is larger but no more than ~ 40 MeV for all the cases.

ergy term is an order of magnetic smaller than that of the CI. Thus, we shall neglect them also in the present study.

C. The scale and renormalization scheme dependence of the decomposition

In the decomposition equation

$$M = \langle H_a \rangle + \langle H_m \rangle + \langle H_g \rangle + \langle H_E \rangle, \quad (18)$$

each of the first two terms and the sum of the last two terms are separately scale and renormalization scheme independent, while each of the last two terms is not.

Another way to decompose the first two terms is to absorb the quark mass anomaly term $\langle H_m^\gamma \rangle$ into the quark mass term $\langle \bar{H}_m \rangle = (1 + \frac{1}{4}\gamma_m)\langle H_m \rangle$, leaving the QCD glue trace anomaly $\langle H_g^a \rangle$ alone. Using Eqs. (46-49) of Ref. [19], we would get the 4-loop result of γ_m in the \overline{MS} scheme at 2GeV to be,

$$\gamma_m^{\overline{MS}}(2\text{GeV}) = 0.26(1). \quad (19)$$

with the uncertainty estimated by its 4th order contribution. The higher order corrections of $\beta(g)$ could also be found in Ref. [19], but this would be beyond the demand of this work since we don't calculate the glue contribution directly. Such a decomposition is not favored, however, as both the total quark mass term and the QCD glue anomaly term depend on both renormalization scheme and scale. It is worthwhile to note that, in the light quark case, the anomaly quark mass term is suppressed by both the quark mass and the factor $\gamma_m/4$ so that the two kinds of decompositions are not significantly different numerically.

For the quark/glue energy, the present calculation of the quark energy is its lattice value at the scale around the inverse of the lattice spacing $a^{-1} = 1.77\text{GeV}$. Since the combined energy is scale and renormalization scheme independent, the glue energy is also at the same scale. In principle, to obtain the result at 2GeV in the \overline{MS} scheme, we could calculate the renormalization of the quark energy in RI/MOM scheme with simulation and then convert it into \overline{MS} scheme perturbatively, or use lattice perturbation theory to calculate the renormalization of the quark energy in \overline{MS} with finite lattice spacing. Also, the mixing effect between the quark/glue components should be taken into account [3, 20].

III. RESULTS

A. The scalar matrix element in the PS/V meson

The CI parts of the matrix element $S_M \equiv \langle M | \int d^3x \bar{\psi}\psi | M \rangle / \langle M | M \rangle$ for PS and V are plotted in Fig. 4. Even though they are almost identical in the heavy quark region as expected, $S_{PS,CI}$

increases with decreasing m_q^R , while $S_{V,CI}$ remains largely constant and is close to unity throughout the quark mass range below the charm quark mass. From the Feynman-Hellman theorem,

$$S_{M,CI} = \frac{\partial M}{\partial m_v}, \quad (20)$$

one can easily deduce the $1/\sqrt{m_q^R}$ behavior of PS mesons with the Gell-Mann-Oakes-Renner relation $m_{PS}^2 = -2m_q \langle \bar{q}q \rangle / f_\pi^2$. We will see later that Eq. (20) is also useful to understand the quark mass dependence of the V meson.

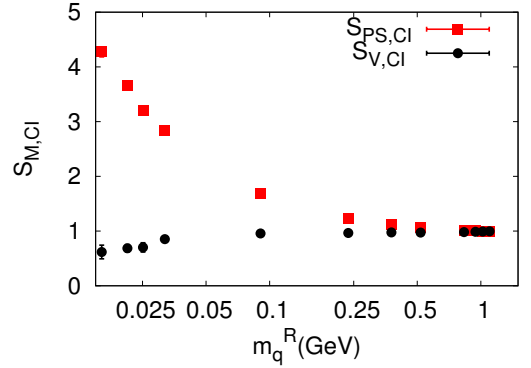


FIG. 4: Matrix elements $S_{M,CI}$ for the PS and V mesons. $S_{PS,CI}$ (red square) increases with decreasing m_q^R while $S_{V,CI}$ (blue circle) remains constant and is close to unity throughout the quark mass range below the charm quark mass.

B. Pseudoscalar meson

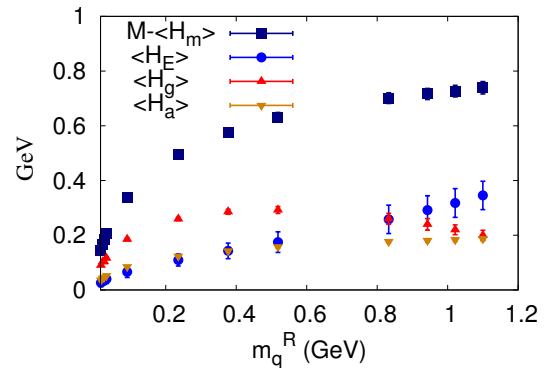


FIG. 5: Different component contributions to the PS mass as functions of the renormalized valence quark mass. The contributions from the glue energy and trace anomaly are stable in the region from 0.2 to 0.8 GeV, while the former one decreases for heavier quark masses.

Our lattice results of the difference between M and the quark mass term $\langle H_m \rangle$, i.e. $M - \langle H_m \rangle$, the quark

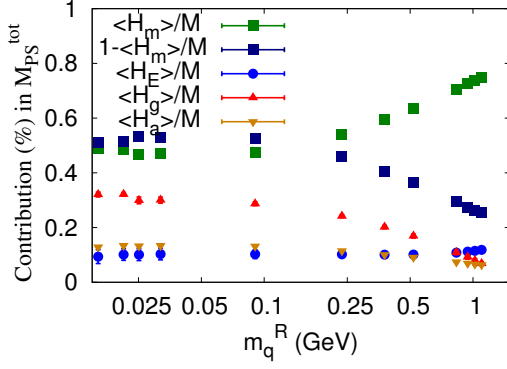


FIG. 6: Ratios of the different component contributions to the PS mass as functions of the renormalized valence quark mass. All these ratios are positive which suggests that all the components approach zero at the chiral limit.

kinetic and potential energy term $\langle H_E \rangle$, the glue field energy $\langle H_g \rangle$, and the anomaly $\langle H_a \rangle$ for the PS meson as a function of the renormalized valence quark mass are presented in Fig. 5. It is interesting to observe that all these contributions are positive which suggests that they all approach zero at the chiral limit when the pion mass approaches zero. We also note that the contributions from the glue energy and trace anomaly are stable in the region of m_q^R from 0.2 to 0.8 GeV and then the former one decreases for the heavier quark mass case.

We also plot the ratios of the quark and glue components with respect to M in Fig. 6. For the light PS mesons, the quark mass term is about 50% of the total mass. This can be derived from the Gell-Mann-Oakes-Renner relation $m_\pi \propto \sqrt{m^q}$ and the Feynman-Hellman relation Eq. (20). This implies from Eq. (12) that the anomaly term $\langle H_a \rangle$ contributes $\sim 12\%$ of the mass. The remaining contributions from $\langle H_g \rangle$ and $\langle H_E \rangle$ are $\sim 30\%$ and $\sim 8\%$ respectively. They are consistent with an estimate based on the quark momentum fraction in the pion and the Gell-Mann-Oakes-Renner relation [2]. Since our present results are from the partially quenched calculation, it will be interesting to check them again in the future for configurations with physical light sea quark masses.

C. Vector meson

The same components in the V mesons and their ratios to the total mass are plotted in Figs. 7 and 8. Close to the chiral limit, $\langle H_E \rangle$ constitutes $\sim 40\%$ of the ρ meson mass, while the sum of the glue energy and anomaly terms contribute about 60% and $\langle H_m \rangle$ vanishes like $O(m_q^R)$.

For the heavier V mesons, the behavior

$$M_V(m_q^R) \sim 2m_q^R C_0 + \text{const.} \quad (21)$$

with C_0 a constant is observed in Fig. 9.

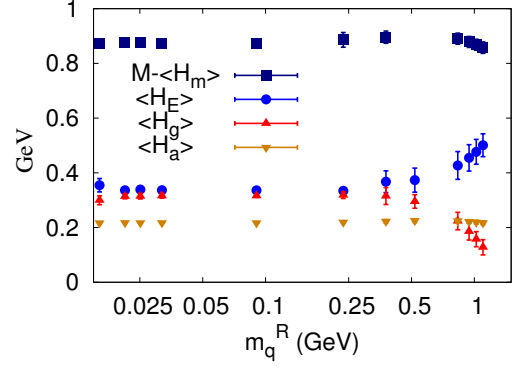


FIG. 7: Same as in Fig. 5 for the vector meson. The contributions from all the components except the quark mass term (which will be discussed in Fig. 8) are stable when the valence quark mass is smaller then ~ 500 MeV.

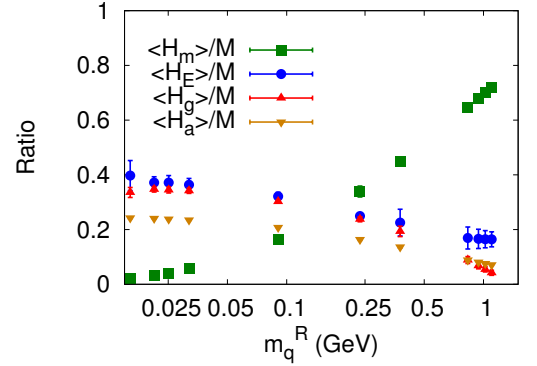


FIG. 8: Same as in Fig. 6 for the vector meson. The quark mass contribution (blue square) increases from almost zero in the light quark region to over 80% in the charm quark region.

We note that the components $\langle H_E \rangle$, $\langle H_g \rangle$ and $\langle H_a \rangle$ are insensitive to the current quark mass through the quark mass region less than ~ 500 MeV. In this region, the glue energy and trace anomaly contribution to the V meson mass, i.e. $\langle H_a \rangle + \langle H_g \rangle$, is about 500 MeV and the quark energy $\langle H_E \rangle$ contributes about 350 MeV. It is tantalizing to consider the possibility that the constant glue contribution and quark energy could be the origin of the constituent quark mass in the quark model picture.

D. Hyperfine splitting

As seen in Fig. 5 and Fig. 7, when the valence quark mass increases, the quark energy contribution also increases while both the glue energy and trace anomaly decrease. To study the consequence of this behavior, we examine the hyperfine splitting of charmonium, we plot in Fig. 10 the difference of the quark and glue components between the V and PS mesons as a function of

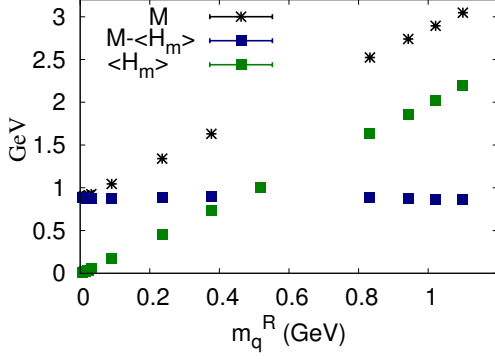


FIG. 9: The quark mass dependence of the V meson mass is linear in the current quark mass and comes mostly from $\langle H_m \rangle$; see their difference marked by the dark blue square.

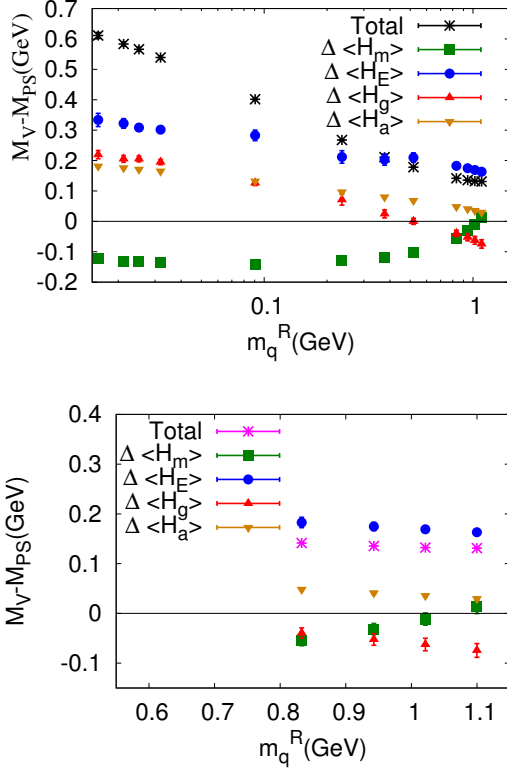


FIG. 10: Contributions to hyperfine splitting for the entire quark mass region (the top panel) and an enlarged plot in the charm quark region (the bottom panel).

the quark mass. For charmonium with m_q^R at 1 GeV, $\Delta\langle H_m \rangle$ is consistent with zero. Therefore, as in Fig. 11, $\Delta\langle H_a \rangle$ gives 1/4 of the hyperfine splitting from the trace anomaly equation Eq. (12). On the other hand, $\Delta\langle H_g \rangle$ turns negative in the charm mass region and largely cancels out the positive $\Delta\langle H_a \rangle$. As a result, the major part of the hyperfine splitting is due to the quark energy difference $\Delta\langle H_E \rangle$. This seems to be consistent with the

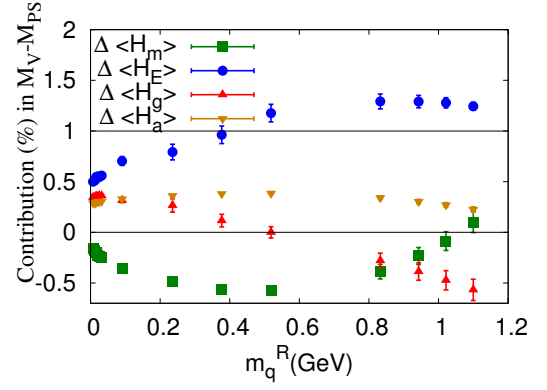


FIG. 11: Contributions to the hyperfine splitting, as portions of the total. In the charm quark mass region, $\Delta\langle H_a \rangle$ (orange reverse triangle) contributes 1/4 since the one from the mass term (green square) is nearly zero. At the same time the contribution from the glue energy difference (red triangle) turns negative, largely canceling the positive $\Delta\langle H_a \rangle$, and leaves the major part of the hyperfine splitting as due to the quark energy difference $\Delta\langle H_E \rangle$ (blue dot).

potential model picture where the charmonium hyperfine splitting is attributable to the spin-spin interaction of the one glue-exchange potential. Higher precision calculation is needed to confirm this.

IV. SUMMARY

In summary, we have directly calculated the quark components of the pseudoscalar and vector meson masses with lattice QCD. The glue field energy and the anomaly components are extracted from the mass relations from the Hamilton and the trace anomaly. We have estimated the systematic errors due to the neglect of the disconnected insertions and the use of equation of motion. From our exploratory study, we confirmed that there are significant contributions from the glue components in light mesons. Throughout the valence quark mass range below the charm, the quark mass dependence of the V meson mass comes almost entirely from $\langle H_m \rangle$, which is linear in the valence quark mass; whereas, $\langle H_E \rangle$, $\langle H_a \rangle$ and $\langle H_g \rangle$ are almost constant. We also find that the hyperfine splitting between J/Ψ and η_c is dominated by the quark energy term.

In the decomposition equation Eq. (18), each of the first two terms and the sum of the last two terms are separately scale and renormalization scheme independent, while each of the last two terms is not. For reference, the scale independent combination of the quark and glue energy contributions to the PS/V meson mass are plotted in Fig. 12. We can see that the combined energy in the V meson is almost a constant (~ 650 MeV), and the one in the PS meson becomes close to that value only in the charm quark region.

For future studies, we will perform calculations with

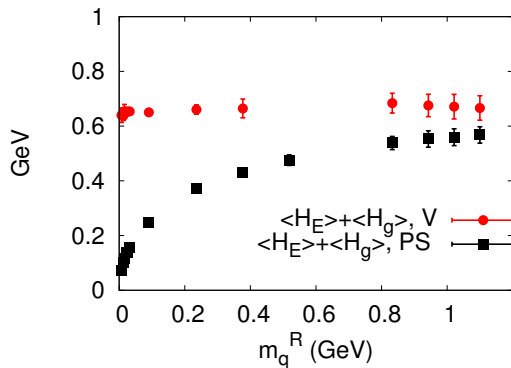


FIG. 12: The combined quark/glue energy contribution to the PS/V meson mass.

the physical sea quark masses and will calculate the glue field energy and trace anomaly contributions directly.

Acknowledgments

We thank RBC and UKQCD Collaborations for providing us their DWF gauge configurations. This work is supported in part by the National Science Foundation of China (NSFC) under Grants No. 11075167, No. 11105153, and No. 11335001, and also by the U.S. DOE Grant No. DE-FG05-84ER40154. Y.C. and Z.L. also acknowledge the support of NSFC and DFG through funds provided to the Sino-German CRC 110 “Symmetries and the Emergence of Structure in QCD”. M. G. and Z. L. are partially supported by the Youth Innovation Promotion Association of CAS (2015013, 2011013).

-
- [1] X.-D. Ji, Phys. Rev. Lett. **74**, 1071 (1995) [hep-ph/9410274].
 - [2] X.-D. Ji, Phys. Rev. **D52**, 271 (1995) [hep-ph/9502213].
 - [3] H. B. Meyer and J. W. Negele, Phys. Rev. D **77**, 037501 (2008) [arXiv:0707.3225 [hep-lat]].
 - [4] S. Caracciolo, G. Curci, P. Menotti and A. Pelissetto, Annals Phys. **197**, 119 (1990).
 - [5] L. Del Debbio and R. Zwicky, Phys. Lett. B **734**, 2014 [arXiv:1306.4274 [hep-ph]].
 - [6] Y. Aoki *et al.* [RBC and UKQCD Collaborations], Phys. Rev. D **83**, 074508 (2011) [arXiv:1011.0892 [hep-lat]].
 - [7] A. Li *et al.* [xQCD Collaboration], Phys. Rev. D **82**, 114501 (2010) [arXiv:1005.5424 [hep-lat]].
 - [8] H. Suzuki, PTEP **2013**, no. 8, 083B03 (2013) [arXiv:1304.0533 [hep-lat]].
 - [9] H. Makino and H. Suzuki, PTEP **2014**, no. 6, 063B02 (2014) [arXiv:1403.4772 [hep-lat]].
 - [10] T.-W. Chiu, Phys. Rev. D **60**, 034503 (1999) [hep-lat/9810052].
 - [11] K.-F. Liu and S.J. Dong, Int. J. Mod. Phys. A **20**, 7241 (2005) [hep-lat/0206002].
 - [12] T.-W. Chiu and S. V. Zenkin, Phys. Rev. D **59**, 074501 (1999) [hep-lat/9806019].
 - [13] Y. B. Yang, Y. Chen, A. Alexandru, S. J. Dong, T. Draper, M. Gong, F. X. Lee, A. Li, K. F. Liu, Z. Liu, and M. Lujan, arXiv:1410.3343 [hep-lat].
 - [14] Z. Liu, Y. Chen, S. J. Dong, M. Glatzmaier, M. Gong, A. Li, K. F. Liu, Y. B. Yang and J. B. Zhang, Phys. Rev. D **90**, 034505 (2014) [arXiv:1312.7628 [hep-lat]].
 - [15] M. Gong *et al.* [XQCD Collaboration], Phys. Rev. D **88**, no. 1, 014503 (2013) [arXiv:1304.1194 [hep-ph]].
 - [16] F. Olness, J. Pumplin, D. Stump, J. Huston, P. M. Nadolsky, H. L. Lai, S. Kretzer and J. F. Owens *et al.*, Eur. Phys. J. C **40**, 145 (2005) [hep-ph/0312323].
 - [17] Mingyang Sun, Yibo Yang, Ming Gong, and Keh-Fei Liu, to be submitted to Proceedings of Lattice Conference 2014.
 - [18] M. A. Shifman, A. I. Vainshtein and V. I. Zakharov, Phys. Lett. B **78**, 443 (1978).
 - [19] K. G. Chetyrkin and A. Retey, Nucl. Phys. B **583**, 3 (2000) [hep-ph/9910332].
 - [20] M. Deka, T. Doi, Y. B. Yang, B. Chakraborty, S. J. Dong, T. Draper, M. Glatzmaier and M. Gong *et al.*, Phys. Rev. D **91**, no. 1, 014505 (2015) [arXiv:1312.4816 [hep-lat]].